

On the Coulomb Breakup of Exotic Nuclei

R. Chatterjee, Shubhchintak

Department of Physics, Indian Institute of Technology, Roorkee, 247667, India

Abstract. We present a fully quantum mechanical theory to study the effects of deformation on various reaction observables in the Coulomb breakup of neutron rich exotic medium mass nuclei on heavy targets within the framework of post-form finite range distorted wave Born approximation by using a deformed Woods-Saxon potential. We study the cases of ^{31}Ne and ^{37}Mg , possible halo candidates in the medium mass region, of the nuclear chart. We also show the utility of using the Coulomb breakup method to investigate the breakdown of shell model magic numbers away from the valley of stability.

1 Introduction

During the past few decades, structures of exotic nuclei have been extensively studied through a number of experiments using radioactive beams. However, it is only recently that one is venturing into medium mass nuclei like ^{23}O , ^{31}Ne and ^{37}Mg . This is a very new and exciting development which has expanded the field of light exotic nuclei to the deformed medium mass region. Venturing away from stability has also given us new insights into long held concepts of nuclear structure - like the magic numbers. Whether they are 'valid' near the drip lines is a very interesting question to pose, given that there are experiments which seems to indicate their breakdown. If so, what are the implications for nuclear astrophysics?

To investigate these phenomena breakup reactions, especially Coulomb breakup of nuclei away from the valley of stability have been one of the most successful probes.

In this writeup we report an extension of the previously proposed [1] theory of Coulomb breakup within the ambit of post-form finite range distorted wave Born approximation (FRDWBA) to include deformations of the projectile in a simple manner [2]. The formalism retains the analytical flavour of the calculation with the transition amplitude being factorized into two parts - the dynamics and the structure part. The structure part contains the deformation parameter and the dynamics part of the problem can be expressed in terms of the Bremsstrahlung integral - which can be analytically evaluated. This has therefore opened a route to investigate the breakup of deformed neutron rich projectiles in the Coulomb field of a heavy target.

The formalism (section 2) is then used to study the Coulomb breakup of ^{31}Ne and ^{37}Mg on heavy targets (Pb and Au) at 234 MeV/u and 240 MeV/u

beam energy, respectively (section 3). Comparing the calculated cross section with the available experimental data, we find the possible ground state spin-parity in both cases. We also study the effect of deformation on various reaction observables in the Coulomb breakup of ^{31}Ne on heavy target at 234 MeV/u beam energy. In section 4, we study the breakdown of $N = 8$ magic number using parallel momentum distribution (PMD) analyses.

2 Formalism

We consider the elastic breakup of a two body composite ‘deformed’ projectile a in the Coulomb field of target t as: $a + t \rightarrow b + c + t$, where projectile a breaks up into fragments b (charged) and c (uncharged). The reduced transition amplitude, $\beta_{\ell m}$, is given by

$$\hat{\ell}\beta_{\ell m}(\mathbf{q}_b, \mathbf{q}_c; \mathbf{q}_a) = \int \int d\mathbf{r}_1 d\mathbf{r}_i \chi_b^{(-)}(\mathbf{q}_b, \mathbf{r}) \chi_c^{(-)}(\mathbf{q}_c, \mathbf{r}_c) V_{bc}(\mathbf{r}_1) \times \phi_a^{\ell m}(\mathbf{r}_1) \chi_a^{(+)}(\mathbf{q}_a, \mathbf{r}_i), \quad (1)$$

where, $\hat{\ell} = \sqrt{2\ell + 1}$, \mathbf{q}_b , \mathbf{q}_c and \mathbf{q}_a are the wave vectors of b , c and a corresponding to Jacobi vectors \mathbf{r} , \mathbf{r}_c and \mathbf{r}_1 , respectively. $\chi_b^{(-)}$ and $\chi_c^{(-)}$ are the distorted waves for relative motions of b and c with respect to t and the center of mass (c.m.) of the $b - t$ system, respectively, with ingoing wave boundary conditions. $\chi_a^{(+)}(\mathbf{q}_a, \mathbf{r}_i)$ is the Coulomb distorted wave of the projectile with outgoing boundary conditions. It describes the relative motion of c.m. of the projectile with respect to the target. Further, $\phi_a^{\ell m}(\mathbf{r}_1) = u_\ell(r_1) Y_{\ell m}(\hat{\mathbf{r}}_1)$ is the ground state wave function of the projectile with relative orbital angular momentum state ℓ and projection m ($u_\ell(r_1)$ is the radial part and $Y_{\ell m}(\hat{\mathbf{r}}_1)$ is the angular part).

$V_{bc}(\mathbf{r}_1)$ [in Eq. (1)] is the interaction between b and c , in the initial channel. This is where we introduce an axially symmetric quadrupole-deformed potential, as

$$V_{bc}(\mathbf{r}_1) = \frac{V_{ws}}{1 + \exp(\frac{r_1 - R}{a})} - \beta_2 R V_{ws} \frac{df(r_1)}{dr_1} Y_2^0(\hat{\mathbf{r}}_1), \quad (2)$$

where V_{ws} is the depth of spherical Woods-Saxon potential, β_2 is the quadrupole deformation parameter. The first part of the Eq. (2) is the spherical Woods-Saxon potential $V_s(r_1)$ with radius $R = r_0 A^{1/3}$. r_0 and a being the radius and diffuseness parameters, respectively. However, to preserve the analyticity of our method, we still calculate the radial part of the ground state wave function of the projectile from undeformed potential V_s . We emphasize that the deformation parameter (β_2) has already entered into the theory via V_{bc} in Eq. (1).

Further, replacing the $\chi_c^{(-)}$ in Eq. (1) by a plane wave [as c is (uncharged)] and expanding the $\chi_b^{(-)}(\mathbf{q}_b, \mathbf{r})$ using the local momentum approximation [1], we get the factorization of the $\beta_{\ell m}$ into two three-dimensional integrals - the

structure part and the dynamics part. The dynamics part remains the same as in Ref. [1], which can be solved analytically in terms of Bremsstrahlung integral. However, the structure part which involves the ground state wave function of the projectile and the effect of deformation is different, which can be simplified analytically to

$$I_f = 4\pi \sum_{l_1 m_1} i^{-l_1} Y_{l_1}^{m_1}(\hat{Q}) \int r_1^2 dr_1 j_{l_1}(Qr_1) u_\ell(r_1) \times \left[V_s \delta_{l_1, \ell} \delta_{m_1, m} - \beta_2 R V_{ws} \frac{df(r_1)}{dr_1} I_1 \right]. \quad (3)$$

where Q is the momentum dependent on the local momentum of the charged fragment and

$$I_1 = \int d\Omega_{r_1} Y_2^0(\hat{r}_1) Y_{l_1}^{m_1^*}(\hat{r}_1) Y_\ell^m(\hat{r}_1),$$

with $|\ell - 2| < l_1 < |\ell + 2|$ and $m_1 = m$. For more details one is referred to Ref. [2].

3 Calculations on Deformed Exotic Nuclei

3.1 ^{31}Ne

^{31}Ne has a low one-neutron separation energy $S_n = 0.29 \pm 1.64$ MeV [3], with a large uncertainty. Its ground state spin-parity (J^π) has been quoted as $3/2^-$ or $1/2^+$ [4], which clearly, is not according to the shell model ordering. Because of large breakup, interaction cross section [4, 5] and low angular momentum of the valance nucleon, it is suggested to be a possible halo nucleus.

In Figure 1, we calculate the one-neutron removal cross section as a function of S_n (left hand side) in the breakup of ^{31}Ne on Pb target at 234 MeV/u beam energy, for three different ground state configurations. The shaded region corresponds to the experimental data from Ref. [4]. It is clear that the configuration corresponding to $J^\pi = 7/2^-$ (dotted line) is unable to reproduce the data at all. So with the present data the possible ground state J^π of ^{31}Ne , as suggested by our calculations, could be $3/2^-$ (solid line) or $1/2^+$ (dot-dashed line). Furthermore, given that a large uncertainty in experimental S_n value, we can put a limit with our calculations, as shown in Figure 1. In the right hand side of Figure 1, we plot the one-neutron removal cross section as a function of β_2 for both the possible ground state configurations $J^\pi = 3/2^-$ (top panel, having solid and dashed lines corresponding to $S_n = 0.29$ MeV and 0.35 MeV, respectively) and $1/2^+$ (bottom panel, with dotted line corresponding to $S_n = 0.35$ MeV). This calculation helps us to narrow down the range of β_2 possible for ^{31}Ne .

From Figure 1, it is clear that the present data cannot completely rule out the possibility of a $1/2^+$ ground state although that would require a very large

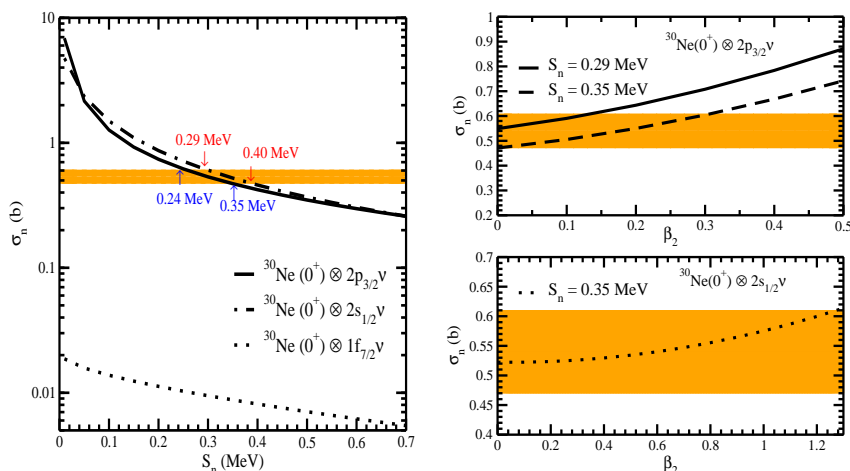


Figure 1. Total cross section in the Coulomb breakup of ^{31}Ne (for $J^\pi = 3/2^-, 1/2^+$ and $7/2^-$) on Pb target at 234 MeV/u beam energy calculated for different values of S_n (left hand side) and for different values of β_2 (right hand side) where, top and bottom panels correspond to $J^\pi = 3/2^-$ and $1/2^+$, respectively. The experimental data shown by the shaded region are from Ref. [4] (for more details, see text).

quadrupole deformation for ^{31}Ne . So, there is a need for calculating more exclusive reaction observables such as relative energy spectra, PMD, neutron angular and energy-angular distributions, in the Coulomb breakup of ^{31}Ne . It is also well known that the peak position of the relative energy spectra depend on the projectile configuration. This can also be seen in Figure 2 (left hand side). Furthermore, the peak height of relative energy spectra depend upon the β_2 (Figure 4 of Ref. [2]). In the right hand side of Figure 2, we plot the PMD of the ^{30}Ne fragment in the Coulomb breakup of ^{31}Ne on Au at 234 MeV/u for $S_n = 0.29$ MeV and for three different values of β_2 [0.0 (solid line), 0.1 (dashed line), 0.3 (dotted line)]. It is clear that the maximum effect of deformation is at peak position and also the full width at half maxima (FWHM) decreases with deformation. For more details and also to see the effect of deformation on other reaction observable such as neutron angular and energy-angular distribution in the Coulomb breakup of ^{31}Ne one is referred to Ref. [2].

3.2 ^{37}Mg

The nucleus of ^{37}Mg too has a large uncertainty in its one-neutron separation energy (0.162 ± 0.686 MeV [6]) and has controversies regarding its ground state spin-parity. Recently measured large breakup cross section [7] and reaction cross section [8] seems to suggest a halo structure in ^{37}Mg .

In Figure 3, we present the one-neutron removal cross section as a function of S_n in the Coulomb breakup of ^{37}Mg on Pb at 240 MeV/u beam energy for

On the Coulomb Breakup of Exotic Nuclei

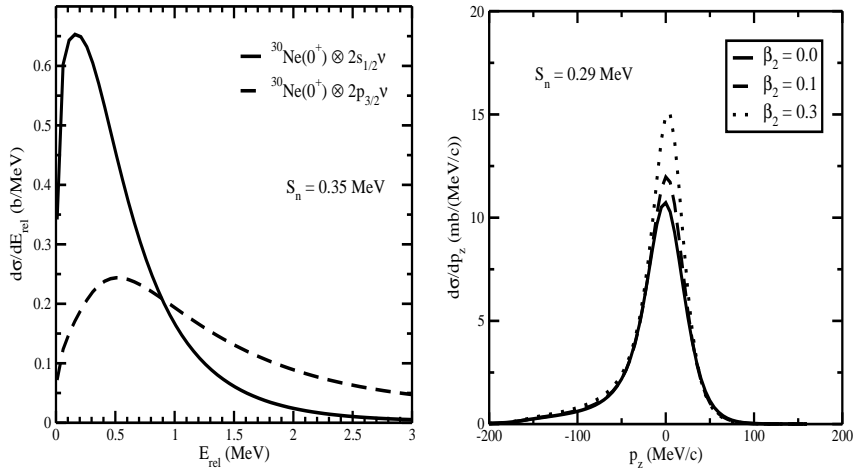


Figure 2. Relative energy spectra in the Coulomb breakup of ^{31}Ne [for $J^\pi = 3/2^-$ (dotted line), $1/2^+$ (solid line)] on Pb target (left hand side) and PMD of charged fragment (^{30}Ne) calculated at three different values of β_2 from breakup on Au target at 234 MeV/u beam energy (right hand side) (for more details, see text).

different possible ground state configurations [$J^\pi = 5/2^-$ (dotted line), $7/2^-$ (dashed line), $3/2^-$ (dot-dashed line) and $1/2^+$ (solid line)]. The shaded region corresponds to the experimental data (preliminary) from Ref. [7]. With the

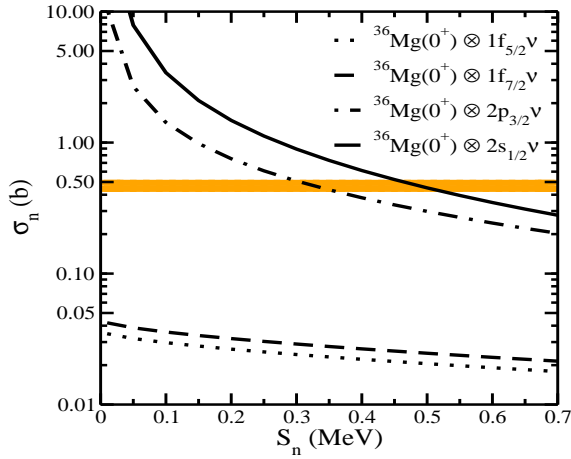


Figure 3. Total cross section in the Coulomb breakup of ^{37}Mg (for $J^\pi = 5/2^-, 7/2^-, 3/2^-$ and $1/2^+$) on Pb target at 240 MeV/u beam energy calculated for different values of S_n . The experimental data (preliminary) shown by the shaded region are from Ref. [7] (for more details, see text).

present data our calculations suggest that possible J^π in this case could be $3/2^-$ or $1/2^+$.

Further calculations of relative energy spectra, momentum and angular distributions, in the breakup of ^{37}Mg on Pb, are in progress and comparison with newly available data (eg. [9]) will help us to reduce the uncertainties in the ground state spin-parity of the nucleus.

4 Breakdown of Magicity and Parallel Momentum Distribution

We now turn our attention to the study of magicity near the $N = 8$ (Be region) as one approaches the neutron drip line from a reaction point of view [10]. The specific reaction observable that we choose is the parallel momentum distribution of the charged fragment, in the Coulomb dissociation of the projectile in the field of a heavy target. Indeed it has been well known that the FWHM of the PMD for the breakup of well known halo nuclei like ^{11}Be and ^{19}C is around 44 MeV/c, while that for stabler isotopes it is around over 140 MeV/c [11, 12]. Our hypothesis is that for the case of magic numbers a larger FWHM should be seen than the neighbouring isotopes.

4.1 Results for $N = 8$ Be isotopes

In Table 1, we present the FWHM from the PMD of the core in the Coulomb breakup of Be isotopes ($N = 5, 6, 7, 8$) on Au target at beam energy of 100 MeV/u, using two models - the FRDWBA as outlined in section 2 (without the deformation part) and the adiabatic model (AD) [13].

Let us now make a few comments on the single particle structure of the Be isotopes considered in Table 1. It is clear from the table that the ground state spin-parity J^π ($3/2^-$) of ^9Be is obtained according to the shell model, where we consider the coupling of $p_{3/2}$ neutron with $^8\text{Be}(0^+)$ core, having threshold energy 1.665 MeV. Interestingly, addition of one more neutron to ^9Be leads to

Table 1. FWHM from the PMD in the Coulomb breakup of Be isotopes on Au at 100 MeV/u beam energy. Shown also are the ground state spin-parities (J^π), ground state single particle configurations, one neutron separation energies (S_n) [14] of the various Be isotopes considered. Note that the FWHM for the breakup of ^{10}Be ($N = 6$) is the highest, rather than ^{12}Be ($N = 8$), having the magic number of neutrons.

Proj- ectile	N	(J^π)	single particle state	S_n (MeV)	FWHM (MeV/c)	
					FRDWBA	AD
^9Be	5	$3/2^-$	$^8\text{Be}(0^+) \otimes 1p_{3/2}\nu$	1.665	112.27	113.87
^{10}Be	6	0^+	$^9\text{Be}(3/2^-) \otimes 1p_{3/2}\nu$	6.812	191.13	170.30
^{11}Be	7	$1/2^+$	$^{10}\text{Be}(0^+) \otimes 2s_{1/2}\nu$	0.501	43.23	43.71
^{12}Be	8	0^+	$^{11}\text{Be}(1/2^+) \otimes 2s_{1/2}\nu$	3.169	88.93	89.73

a tightly bound ^{10}Be nucleus having $^9\text{Be} + n$ separation energy 6.812 MeV. This is an even-even nucleus having $J^\pi = 0^+$ and also follow the normal shell ordering. However, further addition of one more neutron leads to ^{11}Be , which is one of the oldest example of intruder configurations [15], where $2s_{1/2}$ orbital is situated below the $1p_{1/2}$ orbital. This is a well known one-neutron halo nucleus with $S_n = 0.501$ MeV.

The next isotope is ^{12}Be , which corresponds to $N = 8$ shell closure. Its ground state spin suggest that the possible configuration of the last two valance neutrons could be $(p_{1/2})^2$, $(s_{1/2})^2$ or $(d_{5/2})^2$. However, it has been shown in many theoretical as well as experimental studies that there is an admixture of $2s1d$ and $1p$ orbitals in the ground state of ^{12}Be , which is also an indication of the breakdown of $N = 8$ magic number. However, for our calculations we take the dominant single particle configuration, $^{11}\text{Be}(1/2^+) \otimes 2s_{1/2}\nu$, as in Ref. [16]. The $N = 9$ Be isotope (^{13}Be) is known to have only two levels [17], both of which are resonance states with some uncertainties in their positions. Keeping this aside, we shall therefore limit our analyses from $N = 5 - 8$ Be isotopes.

We now turn our attention back to the FWHM calculated in Table 1. The FWHM of the PMD is the smallest for ^{10}Be , which is obtained from the breakup of the well known halo nucleus ^{11}Be . Our calculated results compare quite well with the experimental value of 44 MeV/c [11]. For the case of $N = 8$, experimental results exist for the breakup of ^{12}Be on a light target [16]. Their value of 89 MeV/c (for the s -state) compares quite well with our breakup calculations on a heavy target. It is however interesting to note that the maximum FWHM is obtained for $N = 6$ and not for $N = 8$ (the usual magic number). This is indeed a comment on the breakdown of magicity for $N = 8$ near the drip line.

Let us now return to the central hypothesis of this study. Halo nuclei, which are weakly bound, have a narrow PMD. However if the isotope under consideration has a magic number of neutrons, it is *supposed* be stabler than its neighbouring counterparts. We find it interesting that in the Be chain ^{12}Be ($N = 8$) breakup does not have the largest FWHM. Rather the largest value of FWHM obtained corresponding to $N = 6$ (case of ^{10}Be) suggests that $N = 6$ could be a magic number, which is also in agreement with the studies of Refs. [18, 19].

5 Conclusion

In conclusion, we have extended the quantal theory of Coulomb breakup within the ambit of the FRDWBA to include deformations in projectiles in a simple manner. The formalism retains the analytical flavor of the calculation with the transition amplitude being factorized into two parts – the dynamics and the structure part. The structure part contains the deformation parameter and the dynamics part of the problem can be expressed in terms of the Bremsstrahlung integral – which can be analytically evaluated. This has therefore opened a route to investigate the breakup of deformed neutron rich projectiles in the Coulomb field of a heavy target.

We have also shown the versatility of using the Coulomb breakup method to investigate the breakdown of $N = 8$ magic number away from the stability line.

Acknowledgements

This text presents results from research supported by the Department of Science and Technology, Govt. of India, (SR/S2/HEP-040/2012).

References

- [1] R. Chatterjee, P. Banerjee and R. Shyam, *Nucl. Phys. A* **675** (2000) 477-502; R. Chatterjee, R. Shyam, K. Tsushima, A. W. Thomas, *Nucl. Phys. A* **913** (2013) 116-126.
- [2] Shubhchintak and R. Chatterjee, *Nucl. Phys. A* **922** (2014) 99-111.
- [3] B. Jurado *et al.*, *Phys. Lett. B* **649** (2007) 43-48.
- [4] T. Nakamura *et al.*, *Phys. Rev. Lett.* **103** (2009) 262501-1-4.
- [5] M. Takechi *et al.*, *Mod. Phys. Lett. A* **25** (2010) 1878-1881.
- [6] J. Cameron, J. Chen, B. Singh and N. Nica, *Nucl. Data. Sheets* **113** (2012) 365-514.
- [7] N. Kobayashi *et al.*, *J. Phys: Conf. Series* **436** (2013) 012047-1-3.
- [8] M. Takechi *et al.*, *EPJ Web of Conferences*. **66** (2014) 02101-p.1-p.4.
- [9] N. Kobayashi *et al.*, *Phys. Rev. Lett.* **112** (2014) 242501-1-5.
- [10] Shubhchintak and R. Chatterjee, *Phys. Rev. C* **90** (2014) 017602-1-4.
- [11] J. H. Kelley *et al.*, *Phys. Rev. Lett.* **74** (1995) 30-33.
- [12] E. Sauvan *et al.*, *Phys. Rev.* **C69** (2004) 044603-1-30.
- [13] P. Banerjee, I. J. Thompson, and J. A. Tostevin, *Phys. Rev. C* **58** (1998) 1042-1051.
- [14] <http://www.nndc.bnl.gov/nudat2>.
- [15] I. Talmi and I. Unna, *Phys. Rev. Lett.* **4** (1960) 469-470.
- [16] A. Navin *et al.*, *Phys. Rev. Lett.* **85** (2000) 266-269.
- [17] Y. Kondo *et al.*, *Phys. Lett. B* **690** (2010) 245-249.
- [18] O. Sorlin and M.-G. Porquet, *Prog. Part. Nucl. Phys.* **61** (2008) 602-673.
- [19] T. Otsuka, R. Fujimoto, Y. Utsuno, B. A. Brown, M. Honma, and T. Mizusaki, *Phys. Rev. Lett.* **87** (2001) 082502-1-4.